Model based eversion control of soft growing robots with pneumatic actuation

Enrico Franco

***Abstract*— This letter investigates the model based position control of soft growing robots with pneumatic actuation that extend according to the principle known as eversion. A dynamical model of the system which accounts for the the energy of the ideal gas is presented by employing the port-Hamiltonian formulation. A new control law is constructed with an energy shaping approach. An adaptive observer is employed to compensate the effect of external forces, including that of gravity. Numerical simulations indicate that the proposed controller is superior to simpler energy shaping algorithms.**

***Index Terms*— Emerging control applications, Stability of nonlinear systems, Adaptive control, Soft growing robots.**

I. Introduction

SOFT growing robots are a class of systems capable of navigating the environment without relying on friction with their surroundings [1]. This is achieved by employing a principle known as eversion, according to which a thin-walled tubing extends longitudinally by unfolding its inner membrane [2]. Soft growing robots are typically actuated with compressed air, and they are characterized by a large volume of gas and a comparatively small mass of their rigid parts. Thus the effect of the gas energy on the system dynamics is more pronounced compared to conventional pneumatic drives or to other soft robots. Soft growing robots are employed for inspection of cluttered environments, for search and rescue operations [3], and in a more recent embodiment also for minimally invasive surgery [4]. One of the challenges characterizing soft growing robots is retraction, which requires additional actuators to rewind the inner membrane [5] and can lead to buckling of the tubing [6]. A further challenge is related to steering, which can be achieved by interacting with obstacles [7], by attaching inextensible elements to the tubing thus resulting in pre-set curvature [8], or by using additional actuators [2].

To date few results are available on model based control of soft growing robots [9]. Similarly to other soft robots, kinematic models [10] and kinematic-based controllers can be appropriate if a fast response is not required [8], [11]–[13]. In general however, dynamical models and corresponding model based controllers allow improving the transient performance of soft robots and can compensate the effects of external forces [14], [15]. In addition, accounting for the pressure dynamics can improve the responsiveness of larger soft robots that employ fluidic actuation [16]–[18]. Due to the challenges associated to retracting soft growing robots, avoiding overshoot is highly desirable. In addition, some applications such as search and rescue require high responsiveness, thus resulting in a challenging control problem.

In this letter, the model based control of a soft growing robot with pneumatic actuation is investigated. To this end, a system model that accounts for the energy of the ideal gas and for the effect of external forces is presented by employing a port-Hamiltonian formulation. The main contributions of this work include: i) differently from previous works, both isothermal and polytropic processes are considered, and the effect of pressure on the gas density is accounted for; ii) an extended nonlinear observer is employed to compensate the effect of external forces, including that of gravity due to an unknown slope; iii) a control law is constructed for the resulting model by employing an energy shaping approach with damping assignment, which was not part of [16], [17]; iv) sufficient conditions for global asymptotic stability are provided in relation to the tuning parameters and to some verifiable conditions on the disturbances. Finally, the effectiveness of the controller is demonstrated with numerical simulations and compared with simplified energy shaping algorithms.

The rest of this letter is organized as follows: Section II presents the dynamical model of a soft growing robot; Section III outlines the controller design; Section IV contains the simulation results, and Section V the concluding remarks.

II. Dynamical model

A. Soft growing robot

A soft growing robot typically consists of an inflatable tubular structure that extends at the distal end according to a principle known as eversion [2]. Assuming that the tubing has a uniform section of area A and an everted length $0 \leq x \leq \overline{x}$ measured on its central axis starting from the pressure source, the volume of the pressurized gas is thus $V = Ax + V_0$ (see Figure 1). The internal energy of an ideal gas at the pressure P is given by $\Phi = -\int_{V_0}^{V} P dV$, which computed for a polytropic process with index c yields

$$\Phi = \begin{cases} P(V_0 + Ax) \log\left(\frac{V_0}{V_0 + Ax}\right) & c = 1 \\ -\frac{P(V_0+Ax)^c}{c-1}\left(V_0^{1-c} - (V_0 + Ax)^{1-c}\right) & c \neq 1, \end{cases} \quad (1)$$

where $V_0 = Ax_0$ is the initial volume at $x = 0$. A characteristic of eversion is that, once a portion of the tubing is inflated,

This research was supported by the Engineering and Physical Sciences Research Council (grant EP/W004224/1 and grant EP/R511547/1). Enrico Franco is with the Mechanical Engineering Department, Imperial College London, UK, Exhibition Road, SW7 2AZ. Contacts: e.franco11@imperial.ac.uk.

the outer membrane remains static. Instead, a portion of the inner membrane with length $x + x_0$ travels inside the outer membrane at twice the speed of the tip, that is $2\dot{x}$ [5]. The mechanical energy of the system is thus $H = \frac{1}{2}\dot{x}^2 M_t + \Omega + \Phi$. The mass is $M_t = m + (\rho A + 4\rho_b A_b)(x + x_0) > 0$, where ρ is the gas density and ρ_b is the density of the tubing, while m is the mass of the tool at the tip. In particular, $\rho = \rho_0 \frac{P^{1/c}}{P_a^{1/c}}$, where ρ_0 is the gas density at the atmospheric pressure P_a. The potential energy due to gravity associated to the whole everted length is $\Omega(x) = g\int_0^x M_t(\hat{x})h(\hat{x})d\hat{x}$. While the height $h(x)$ might not be measurable during locomotion on unknown terrains, it is bounded by the length x, that is $|h(x)| \leq |x|$. Assuming that the robot moves on a constant slope $h(x) = h_0 x$ yields $\Omega(x) = \left(F_{10} + F_{11}\frac{P^{1/c}}{P_a^{1/c}}\right)\frac{x^2}{2} + \left(F_{20} + F_{21}\frac{P^{1/c}}{P_a^{1/c}}\right)\frac{x^3}{3}$, where $F_{10} = gh_0(m + 4A_b\rho_b x_0), F_{11} = gh_0 A\rho_0 x_0, F_{20} = 4gh_0 A_b\rho_b, F_{21} = gh_0 A\rho_0$. Accounting for the effect of the external forces δ in the direction of motion, the system dynamics in port-Hamiltonian form is

$$\begin{bmatrix}\dot{x}\\ \dot{p}\\ \dot{P}\end{bmatrix} = \begin{bmatrix}0 & 1 & 0\\ -1 & -b & \frac{\Gamma_0 A}{V}\\ 0 & -\frac{\Gamma_0 A}{V} & 0\end{bmatrix}\begin{bmatrix}\partial_x H\\ \partial_p H\\ \partial_P H\end{bmatrix} + \begin{bmatrix}0\\ -\delta\\ \frac{cR_sT}{V}Q\end{bmatrix}, \quad (2)$$

where the system states are the position $x \in \mathbb{R}$, the momenta $p = M_t\dot{x}$, and the pressure P. The bulk modulus of a fluid is defined as $\Gamma_0 = -V\frac{\partial P}{\partial V}$, which for an ideal gas with polytropic index c yields $\Gamma_0 = cP$. The physical damping is b, the gas constant is R_s, and Q is the mass flow rate of gas flowing into the tubing. The notation $\partial_x H = \frac{\partial H}{\partial x}, \partial_p H = \frac{\partial H}{\partial p}, \partial_P H = \frac{\partial H}{\partial P}$ is employed throughout the paper for conciseness.

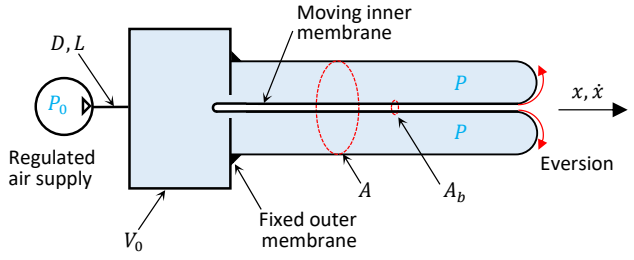

Fig. 1. Schematic of soft growing robot: section view with system states and key model parameters. For simplicity, no tool is shown at the tip.

The following assumptions are introduced for controller design purposes.

Assumption 1: The gas is ideal and has a polytropic index c and a specific constant R_s; the pressure P of the gas, its density ρ, and its speed $\dot{x}$ are uniform in the volume V.

Assumption 2: The tip position x, its time derivative $\dot{x}$, and the pressure P are known at any instant; in addition x and P are bounded, that is $0 \leq x \leq \overline{x}$ and $P_a \leq P \leq \overline{P}$.

Assumption 3: The potential energy is $\Omega(x) = \left(F_{10} + F_{11}\frac{P^{1/c}}{P_a^{1/c}}\right)\frac{x^2}{2} + \left(F_{20} + F_{21}\frac{P^{1/c}}{P_a^{1/c}}\right)\frac{x^3}{3}$ where the terms F_{10}, F_{11}, F_{20} and F_{21} are unknown but bounded and constant.

Assumption 4: The external forces $\delta = AP_a + F_0 + F_3\dot{x}$ are bounded, where $F_0 > 0$ and $F_3 > 0$ are unknown but constant. All remaining model parameters are known.

The parameterization chosen for δ and Ω describes the so-called path-independent eversion forces [19]: i) the yield pressure below which no growth occurs is accounted for by F_0; ii) internal and external viscous friction are accounted for by F_3 and by the physical damping b; iii) besides contributing to Ω, F_{10} is also representative of length-dependent static friction. It follows from *Assumptions 3* and *4* that the vector $F = [F_0, F_{10}, F_{11}, F_{20}, F_{21}, F_3]$ is bounded, that is $|F| \leq \overline{F}$. Note that the model (2) is specific to unconstrained growth by eversion, while steering and retraction are not considered. This is motivated by the fact that growth by eversion, steering, and retraction are typically actuated independently [9].

B. Regulated air supply

The flow rate through an equivalent orifice with conductance C depends on the upstream pressure P_0 and on the downstream pressure P according to ISO 6358

$$Q = \begin{cases} P_0 C\sqrt{1 - \left(\frac{\frac{P}{P_0} - \epsilon}{1-\epsilon}\right)^2} & \epsilon < \frac{P}{P_0} < 1\\ P_0 C & 0 < \frac{P}{P_0} \leq \epsilon\\ -PC\sqrt{1 - \left(\frac{\frac{P_0}{P} - \epsilon}{1-\epsilon}\right)^2} & \epsilon < \frac{P_0}{P} < 1\\ -PC & 0 < \frac{P_0}{P} \leq \epsilon, \end{cases} \quad (3)$$

where $\epsilon = 0.528$ is the critical pressure ratio for an ideal gas, corresponding to sonic flow [20]. In the proposed setup, compressed air is supplied through a pipe by a digital pressure regulator hence P_0 represents the control input for system (2), while the internal pressure P is a system state. It follows from (3) that the flow rate could be either positive for inflow or negative for outflow. Computing P_0 from (3) gives

$$P_0 = \begin{cases} P\epsilon\frac{1-\sqrt{1-\left(2-\frac{1}{\epsilon}\right)\left(1+\frac{Q^2}{(CP)^2}(1-\epsilon)^2\right)}}{2\epsilon - 1} & \epsilon < \frac{P}{P_0} < 1, Q > 0\\ \frac{Q}{C} & 0 < \frac{P}{P_0} \leq \epsilon, Q > 0\\ P\left(\epsilon + (1-\epsilon)\sqrt{1 - \frac{Q^2}{(CP)^2}}\right) & -CP < Q < 0\\ P\epsilon & Q < -CP. \end{cases} \quad (4)$$

Finally, the conductance of an orifice of diameter D and length L at the outlet of the pressure regulator is given by

$$C = \frac{0.029D^2}{\sqrt{\frac{L}{D^{1.25}} + 510}}. \quad (5)$$

III. Model Based Position Control

The control aim is to regulate the position of the tip to $x = x^*$ only by acting on the pressure P_0. This goal has typically been achieved with the combination of pressure to produce growth and of an additional motor pulling the inner membrane to resist growth and avoid overshoot [9].

A. Nonlinear observer

A nonlinear observer is constructed by employing the *Immersion and Invariance* methodology [21] to estimate the

vector $F = [F_0, F_{10}, F_{11}, F_{20}, F_{21}, F_3]$. To this end define the vector of estimation errors $z_F = [z_0, z_{10}, z_{11}, z_{20}, z_{21}, z_3]^T$ as

$$z_F = \hat{F} + \beta_F - F, \tag{6}$$

where $\beta_F = [\beta_0, \beta_{10}, \beta_{11}, \beta_{20}, \beta_{21}, \beta_3]^T$ are functions of the system states (x, p, P), while $\hat{F} = [\hat{F}_0, \hat{F}_{10}, \hat{F}_{11}, \hat{F}_{20}, \hat{F}_{21}, \hat{F}_3]^T$ are the observer states. The vector F is thus approximated with $\hat{F} + \beta_F$.

Proposition 1: Consider system (2) with *Assumptions 1* to *4* and the functions

$$\begin{aligned} \beta_F &= -\alpha p \begin{bmatrix} 1 & x & \kappa_1 \frac{P^{1/c}}{P_a^{1/c}} & x^2 & \kappa_2 \frac{P^{1/c}}{P_a^{1/c}} & \frac{p}{2M_t} \end{bmatrix}^T, \\ \kappa_1 &= \frac{x^2 + 2xx_0}{2x + 2x_0}, \ \kappa_2 = \frac{2x^3 + 3x^2 x_0}{3x + 3x_0}, \end{aligned} \tag{7}$$

$$\begin{aligned} \dot{\hat{F}} &= -\partial_x \beta_F \frac{p}{M_t} - \partial_P \beta_F \dot{P} + \partial_p \beta_F \left(b \frac{p}{M_t} \right) \\ &+ \partial_p \beta_F \left(\Omega_F (\hat{F} + \beta_F) - A(P - P_a) - 2\rho_b A_b \frac{p^2}{M_t^2} \right), \\ \Omega_F &= \begin{bmatrix} 1 & x & \kappa_1 \frac{P^{1/c}}{P_a^{1/c}} & x^2 & \kappa_2 \frac{P^{1/c}}{P_a^{1/c}} & \frac{p}{M_t} \end{bmatrix}. \end{aligned} \tag{8}$$

Then the quantity $\eta = \Omega_F z_F$ is bounded and converges to zero asymptotically for all $\alpha > 0$, provided that the system trajectories are bounded in closed loop with the control law.

Proof: Computing $\dot{p}$ and $\dot{P}$ from (2) yields

$$\begin{aligned} \dot{p} &= A(P - P_a) - b \frac{p}{M_t} - \Omega_F \left(\hat{F} + \beta_F \right) + \eta + 2\rho_b A_b \frac{p^2}{M_t^2}, \\ \dot{P} &= \frac{QcR_sT}{A(x + x_0)} - \frac{cPp}{(x + x_0)M_t}. \end{aligned} \tag{9}$$

Computing the time derivative of (6) and substituting (9) yields

$$\begin{aligned} \dot{z_F} &= \dot{\hat{F}} + \partial_x \beta_F \frac{p}{M_t} + \partial_p \beta_F \left(AP + 2\rho_b A_b \frac{p^2}{M_t^2} + \eta \right) \\ &- \partial_p \beta_F \left(AP_a + b \frac{p}{M_t} + \Omega_F \left(\hat{F} + \beta_F \right) \right) + \partial_P \beta_F \dot{P}. \end{aligned} \tag{10}$$

Substituting (7), (8) into (10), where $\partial_p \beta_F = -\alpha \Omega_F$, yields $\dot{z_F} = -\alpha \Omega_F^T \Omega_F z_F$. Defining the storage function $\Psi = \frac{1}{2} z_F^T z_F$ and computing its time derivative yields $\dot{\Psi} = -\alpha \eta^2 \leq 0$ for all $\alpha > 0$, thus $\eta \in \mathcal{L}^2$ and $z_F \in \mathcal{L}^\infty$. If (x, p, P) and their time derivatives are bounded in closed loop, it follows that $\dot{z_F} \in \mathcal{L}^\infty$, and thus $\eta, \dot{\eta} \in \mathcal{L}^\infty$. Consequently, η is bounded and converges to zero asymptotically [22] □

B. Control law

The control law is designed by extending the energy shaping approach [23] with a similar procedure to [16], [17] such that the closed-loop dynamics in port-Hamiltonian form becomes

$$\begin{bmatrix} \dot{x} \\ \dot{p} \\ \dot{P} \end{bmatrix} = \begin{bmatrix} 0 & S_{12} & S_{13} \\ -S_{12} & -S_{22} & S_{23} \\ -S_{13} & -S_{23} & -S_{33} \end{bmatrix} \begin{bmatrix} \partial_x H_d \\ \partial_p H_d \\ \partial_P H_d \end{bmatrix} + \begin{bmatrix} 0 \\ \eta \\ 0 \end{bmatrix}, \tag{11}$$

where $H_d = \Omega_d + \frac{1}{2} \frac{p^2}{M_d} + \frac{1}{2} \varsigma^2$ is a positive definite storage function. In particular, $\Omega_d = \frac{1}{2} k_p (x - x^*)^2$ with $k_p > 0$ satisfies the minimizer condition $x^* = \operatorname{argmin}(\Omega_d)$. Differently from [16], [17], the controller design includes damping assignment through a parameter k_v and the mass M_d is set constant rather than proportional to M_t, thus ς is defined in the more general form

$$\begin{aligned} \varsigma &= A(P - P_a) + 2\rho_b A_b \frac{p^2}{M_t^2} + k_v \frac{p}{M_t} \\ &+ \frac{M_d}{M_t} k_p (x - x^*) - \Omega_F \left(\hat{F} + \beta_F \right). \end{aligned} \tag{12}$$

Since (12) contains the nonlinear observer (7) and (8), the term η appears in (11). The terms S_{ij} in (11) are defined as

$$\begin{aligned} S_{12} &= \frac{M_d}{M_t}, \ S_{13} = -\frac{M_d}{M_t} \frac{\partial_p \varsigma}{\partial_P \varsigma}, \ S_{22} = \frac{M_d}{M_t} (b + k_v), \\ S_{23} &= \frac{1 + \frac{M_d}{M_t} \partial_x \varsigma + \frac{M_d}{M_t} (b + k_v) \partial_p \varsigma}{\partial_P \varsigma}, \ S_{33} = k_i, \end{aligned} \tag{13}$$

where k_p, k_i, k_v are tuning parameters. The control input is

$$\begin{aligned} Q &= \frac{PAp}{R_s T M_t} - \frac{A(x + x_0)}{cR_s T} S_{13} \left(k_p (x - x^*) + \varsigma \partial_x \varsigma \right) \\ &- \frac{A(x + x_0)}{cR_s T} \left(S_{23} \left(\frac{p}{M_d} + \varsigma \partial_p \varsigma \right) + S_{33} \varsigma \partial_P \varsigma \right), \end{aligned} \tag{14}$$

where S_{13}, S_{23}, S_{33} are given in (13). The regulated pressure P_0 is then computed from (4).

Proposition 2: Consider system (2) with *Assumptions 1* to *4* in closed-loop with the control law (14) and the observer (7),(8). Assume that there exist some k_p, M_d, α and k_v such that $\partial_P \varsigma \neq 0$ for a given $\overline{F}$. Define then the positive constant parameters $k_i, M_d, k_v, k_p, \alpha$ such that

$$\Theta = \begin{bmatrix} \frac{M_d}{M_t}(b + k_v) & -\frac{1}{2} & 0 \\ -\frac{1}{2} & \alpha & 0 \\ 0 & 0 & k_i (\partial_P \varsigma)^2 \end{bmatrix}, \tag{15}$$

is positive definite. Sufficient conditions for k_i, M_d, k_v, α are

$$\begin{aligned} k_v &> \frac{b\rho_0 A}{4\rho_b A_b} \frac{P^{1/c}}{P_a^{1/c}} + \frac{mb}{4\rho_b A_b k_m \alpha} + k_v' \frac{\rho_b A_b k_m}{b M_d} > 0, \\ M_d &> \rho_b A_b \frac{k_m}{b}, \ k_m > 0, \ k_i > 0, \ \alpha k_m > \overline{x} + x_0. \end{aligned} \tag{16}$$

Then the equilibrium $x = x^*$ is globally asymptotically stable.

Proof: Note first that substituting the control law (14) into (2) yields (11) with the parameters (13), thus the following matching equations are verified

$$\frac{p}{M_t} = S_{12} \frac{p}{M_d} + S_{12} \varsigma \partial_p \varsigma + S_{13} \varsigma \partial_P \varsigma, \tag{17}$$

$$\begin{aligned} &A(P - P_a) + 2\rho_b A_b \frac{p^2}{M_t^2} - b \frac{p}{M_t} - \Omega_F \left(\hat{F} + \beta_F \right) + \eta = \\ &S_{23} \varsigma \partial_P \varsigma - S_{22} \left(\frac{p}{M_d} + \varsigma \partial_p \varsigma \right) - S_{12} \left(k_p (x - x^*) + \varsigma \partial_x \varsigma \right), \end{aligned} \tag{18}$$

$$\begin{aligned} &\frac{QcR_sT}{A(x + x_0)} - \frac{cPp}{(x + x_0)M_t} = -S_{33} \varsigma \partial_P \varsigma \\ &- S_{23} \left(\frac{p}{M_d} + \varsigma \partial_p \varsigma \right) - S_{13} \left(k_p (x - x^*) + \varsigma \partial_x \varsigma \right). \end{aligned} \tag{19}$$

Defining the Lyapunov function $\Upsilon = \Psi + H_d$ and computing its time derivative along the trajectories of the closed-loop system (11) while substituting $\dot{\Psi}$ from *Proposition 1* yields

$$\begin{aligned}\dot{\Upsilon} = -\frac{M_d}{M_t}\left(b + k_v\right)\left(\partial_p H_d\right)^2 + \partial_p H_d \eta \\ -\alpha\eta^2 - k_i(\partial_P \varsigma)^2 \varsigma^2.\end{aligned} \tag{20}$$

Refactoring common terms in (20) yields

$$\dot{\Upsilon} = -y^T \Theta y, \tag{21}$$

where $y^T = \begin{bmatrix}\partial_p H_d & \eta & \varsigma\end{bmatrix}$ with $\partial_p H_d = \frac{p}{M_d} + \varsigma \partial_p \varsigma$ while Θ is given in (15). Thus $\dot{\Upsilon} \leq 0$ and the equilibrium is stable provided that $k_i > 0, \partial_P \varsigma \neq 0$ and $\frac{M_d}{M_t}(b + k_v)\alpha > \frac{1}{4}$. In particular $p, \varsigma \in \mathcal{L}^2 \cap \mathcal{L}^\infty$ and $\eta \in \mathcal{L}^2$, while $z_F, P, x \in \mathcal{L}^\infty$. Since all states are bounded in closed loop, it follows from *Proposition 1* that η converges to zero.

To compute the lower bound of k_v in (16) substitute M_t in (15) which yields the inequality

$$M_d(b + k_v)\alpha > \frac{m}{4} + \left(\frac{\rho_0 A}{4}\frac{P^{1/c}}{P_a^{1/c}} + \rho_b A_b\right)(x + x_0), \tag{22}$$

where $0 \leq x \leq \overline{x}, P_a \leq P \leq \overline{P}$. Setting $M_d = \rho_b A_b \frac{k_m}{b} > 0$ for some $k_m > 0$ and $k_v > \frac{b\rho_0 A}{4\rho_b A_b}\frac{P^{1/c}}{P_a^{1/c}} + \frac{mb}{4\rho_b A_b k_m \alpha} + k_v^{'}\frac{\rho_b A_b k_m}{b M_d}$ with $k_v^{'} > 0$, (22) is verified for all $x + x_0 \leq \alpha k_m$. Thus a conservative choice of α and k_m is $\alpha k_m \geq x_0 + \overline{x}$. It remains to show that $\partial_P \varsigma \neq 0$ for some k_p, M_d, k_v, α and $\overline{F}$. Computing $\partial_P \varsigma$ from (12) yields

$$\begin{aligned}\partial_P \varsigma = -\frac{\rho_0 A}{P}(x + x_0)\left(4\rho_b A_b \frac{p^2}{M_t^3} + k_v \frac{p}{M_t^2}\right)\frac{P^{1/c}}{P_a^{1/c}} \\ + A + \frac{\rho_0 A}{P} k_p \frac{M_d}{M_t^2}(x^* - x)(x + x_0)\frac{P^{1/c}}{P_a^{1/c}} \\ -\partial_P \Omega_F\left(\hat{F} + \beta_F\right) - \Omega_F \partial_P \beta_F.\end{aligned} \tag{23}$$

Since $\dot{\Upsilon} \leq 0$, the system's trajectory starting at $\Upsilon(t_0)$ descends to lower level sets, that is $\Omega_d + \frac{1}{2}\frac{p^2}{M_d} + \frac{1}{2}\varsigma^2 + \frac{1}{2} z_F^T z_F \leq \Upsilon(t_0)$, where $z_F(t_0) = \overline{F}$. Consequently the upper bound of p is $\overline{p} = \sqrt{2 M_d \Upsilon(t_0)}$. The upper bounds of z_F and $\hat{F}$ can be computed in a similar fashion, while the bounds of x and P are known from *Assumption 2*. Substituting $\overline{p}$ and $\overline{\hat{F}}$ in (23) and imposing $\partial_P \varsigma > 0$ yields an inequality which can be evaluated in advance for all $0 \leq x \leq \overline{x}, P_a \leq P \leq \overline{P}$ given k_p, M_d, α and k_v. Considering for illustrative purposes $(x, p, P, \hat{F}) = (0, \overline{p}, P_a, \overline{\hat{F}})$ with $c \neq 1$ and rearranging terms in (23) gives

$$\begin{aligned}\left(-k_p M_d x^* + 4\rho_b A_b \frac{\overline{p}^2}{M_t} + k_v \overline{p}\right)\frac{\rho_0 x_0}{M_t^2} \\ + \left(\frac{\overline{p}\overline{\hat{F}}}{c}(m + A\rho_0 x_0 + A_b \rho_b x_0) - \alpha\frac{\overline{p}^3}{c}\right)\frac{\rho_0 x_0}{M_t^2} < P_a,\end{aligned}$$

which is verified by the sufficient condition

$$\begin{aligned}k_p M_d x^* + \frac{\alpha \overline{p}^3}{c} \geq \frac{4\rho_b A_b \overline{p}^2}{M_t} + \\ \frac{\overline{p}\overline{\hat{F}}\left(m + x_0\left(A\rho_0 + A_b\rho_b\right)\right)}{c} + k_v \overline{p}.\end{aligned}$$

To prove asymptotic stability of the equilibrium, note that $y = 0$ is the set of points where $\dot{\Upsilon} = 0$ and it implies $\dot{p} = p = 0, \varsigma = 0$, and $\eta = 0$. Computing $\dot{p}$ from (11) at $y = 0$ yields $k_p(x^* - x) = 0$. Thus the equilibrium $x^* = \text{argmin}(\Omega_d)$ is the largest invariant set in $y = 0$ and it is asymptotically stable (see Corollary 3.1 in [24]). Finally, computing (12) at $p = \varsigma = 0$ and $x = x^*$ yields the pressure at the equilibrium, that is $P^* = P_a + \Omega_F(\hat{F} + \beta_F)/A$.

To prove the global claim we proceed to show that H_d (and therefore Υ) is radially unbounded (see Corollary 3.2 in [24]). To this end note that $H_d, z_F \to \infty \implies \Upsilon \to \infty$ and $x, p, \varsigma \to \infty \implies H_d \to \infty$. In addition, it follows from (12) that $P \to \infty \implies \varsigma \to \infty \implies H_d \to \infty$, while $\varsigma = 0 \implies AP = -2\rho_b A_b \frac{p^2}{M_t^2} + AP_a - k_v \frac{p}{M_t} - \frac{M_d}{M_t} k_p (x - x^*) + \Omega_F\left(\hat{F} + \beta_F\right)$. Consequently, the condition $\varsigma = 0 \cap P \to \infty$ requires either $q \to \infty$ or $p \to \infty$, which yield finally $H_d \to \infty$ concluding the proof $\square$

Remark 1: The external force F_3 acts on the system dynamics (2) in a similar way to the damping b. Thus F_3 can either be accounted for by $\Omega_F\left(\hat{F} + \beta_F\right)$ in ς as done in (12), or alternatively alongside b in S_{23} and in (15), that is

$$\begin{aligned}S_{22} = \frac{M_d}{M_t}\left(b + k_v + \hat{F}_3 + \beta_3\right), \\ S_{23} = \frac{1 + \frac{M_d}{M_t}\partial_x \varsigma + \frac{M_d}{M_t}\left(b + k_v + \hat{F}_3 + \beta_3\right)\partial_p \varsigma}{\partial_P \varsigma}.\end{aligned} \tag{24}$$

The resulting control law still depends on $\hat{F}_3 + \beta_3$ but it does not compensate this effect, thus yielding a slower response.

Remark 2: Approximating the density of the gas with the constant value ρ_0 simplifies the nonlinear observer since $\Omega(x) = F_{10}\frac{x^2}{2} + F_{20}\frac{x^3}{3}$ where $F_{10} = g h_0(m + x_0(\rho_0 A + 4\rho_b A_b)), F_{20} = g h_0(\rho_0 A + 4\rho_b A_b)$ thus

$$\begin{aligned}\Omega_F = \begin{bmatrix}1 & x & x^2 & \frac{p}{M_t}\end{bmatrix}, \\ \beta_F = -\alpha p \begin{bmatrix}1 & x & x^2 & \frac{p}{2M_t}\end{bmatrix}^T.\end{aligned} \tag{25}$$

Setting $M_d = k_m M_t$ for some $k_m > 0$ and $k_v = 0$ recovers the controller design [17] as a special case, that is

$$\varsigma = A(P - P_a) + k_p k_m (x - x^*) - \Omega_F\left(\hat{F} + \beta_F\right), \tag{26}$$

$$\begin{aligned}S_{12} = k_m,\ S_{13} = 0,\ S_{22} = k_m b, \\ S_{23} = \frac{1 + k_m \partial_x \varsigma + k_m b \partial_p \varsigma}{A},\ S_{33} = k_i.\end{aligned} \tag{27}$$

Note that ς in (26) does not depend on p thus $S_{13} = 0$, while Ω_F does not depend on P hence $\partial_P \varsigma = A$. A further difference from [17] is that system (2) is fully actuated, thus the controller (14) does not require solving any PDE.

Remark 3: Neglecting the pressure dynamics altogether by assuming $P_0 = P$ in (2) further simplifies the control law and the nonlinear observer (8) as

$$P_0 = P_a + \frac{\Omega_F}{A}\left(\hat{F} + \beta_F\right) - \frac{k_p k_m}{A}(x - x^*) - k_v \frac{p}{A M_t}, \tag{28}$$

$$\dot{\hat{F}} = \partial_p \beta_F\left(\frac{bp}{M_t} - A(P_0 - P_a) + \Omega_F(\hat{F} + \beta_F)\right) - \partial_x \beta_F \frac{p}{M_t}. \tag{29}$$

IV. Simulation Results

The system (2) has been simulated in MATLAB using an ODE23 solver and employing the model parameters in SI units $A = 4.9 \times 10^{-4}, A_b = 3 \times 10^{-6}, V_0 = 10^{-3}, c = 1.5, \rho_0 = 1.225, \rho_b = 900, \epsilon = 0.528, R_s = 287, T = 293, D = 4 \times 10^{-3}, L = 10^{-2}, b = 1, m = 0.1, P_a = 10^5$ for illustrative purposes, which correspond to air undergoing adiabatic expansion in a polythene tubing of diameter 25 mm and thickness 0.06 mm. With the former parameters, the mass of air accounts for approximately 14% of the total mass M_t thus neglecting its effect on the dynamics can compromise performance. The unknown external forces have been set as $F_0 = 0.2(1 + \tanh(\dot{x}))$ and $F_3 = 0.5$ corresponding respectively to a smooth approximation of the yield pressure, and to viscous friction. Both values are comparable in magnitude to those reported in [19]. The unknown slope is defined for illustrative purposes as either $h_0 = 0.4$, which is indicated as h_1, or $h_0 = 0.5 + 0.2\sin(4\pi x)$, which is indicated as h_2, or as $h_0 = 0.5 - 0.6\sin(4\pi x)$, which is indicated as h_3. The tuning parameters of the controller (14) and of the observer (7) and (8) have been chosen as $k_p = 1, k_v = 1, k_i = 1, M_d = 2.5m$ and $\alpha = 5$, which satisfy the conditions in *Proposition 2*. Finally, the regulated pressure P_0 is computed with (4).

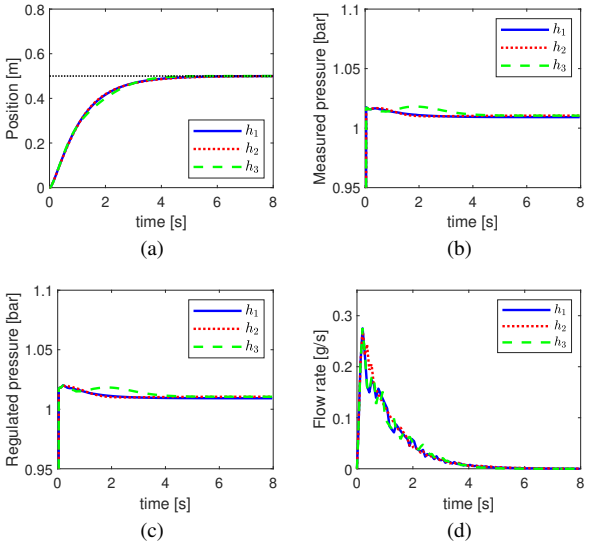

Fig. 2. Simulation results for system (2) with controller (14) and observer (7),(8) for different slopes: (a) tip position $\boldsymbol{x}$; (b) measured pressure $\boldsymbol{P}$; (c) regulated pressure $\boldsymbol{P_0}$; (d) mass flow rate $\boldsymbol{Q}$.

Figure 2 shows the time history of the states x, P, the regulated pressure P_0, and the flow rate Q with controller (14) for the different slopes. In all cases the regulation goal $x^* = 0.5$ is achieved in approximately 5 seconds without overshoot, while the transient remains smooth for both position and pressure. Employing the implementation outlined in *Remark 1* yields similar results which are omitted for brevity.

Figure 3 shows the time history of the states x, P and of P_0 and Q for the slope h_3 while considering different values of the parameter A in the model (2). The controller (14) is compared to the simplified energy shaping designs discussed in *Remark 2* and in *Remark 3* using the tuning parameters $k_p = 1, k_m = 2, k_v = 1, k_i = 1, \alpha = 5$ in both cases for consistency. All controllers yield similar performance with a small A and the regulation goal is achieved in approximately 5 seconds. Employing larger values of A, which correspond to polythene tubing of diameter 50 mm and 60 mm respectively, can result in performance degradation or in higher control effort with the simplified energy shaping controllers. This can be explained considering that assuming constant density of the gas $\rho = \rho_0$ as in *Remark 2* or neglecting it altogether as in *Remark 3* underestimates the inertia of the system. In particular, the controller outlined in *Remark 2* does not show noticeable performance degradation but it requires a higher control input and a higher regulated pressure compared to the controller (14). The controller outlined in *Remark 3* shows a more severe performance degradation even though the regulated pressure and the flow rate remain comparatively low. This is expected since neglecting the pressure dynamics is known to degrade performance [18]. No overshoot is observed with the controller (14) and the transient is consistent across all conditions highlighting the advantages of this approach.

V. Conclusion

In this letter, the dynamical model of a soft growing robot with pneumatic actuation that accounts for the energy of the ideal gas has been presented by employing the port-Hamiltonian formulation. A nonlinear control law has been constructed with an energy-shaping and damping-assignment approach, and the effect of a class of unknown external forces, including gravity due to eversion on an unknown constant slope, has been compensated with a nonlinear observer. The simulation results indicate that the proposed controller achieves the regulation goal in a consistent fashion and without overshoot for different slopes. In comparison, simpler energy shaping controllers can lead to overshoot in some conditions. Future work will aim to further relax the initial assumptions, to investigate simultaneous eversion and steering control, and to conduct experimental tests on a prototype.

References

[1] E. W. Hawkes, L. H. Blumenschein, J. D. Greer, and A. M. Okamura, "A soft robot that navigates its environment through growth," *Science Robotics*, vol. 2, p. 3028, 7 2017.

[2] J. D. Greer, T. K. Morimoto, A. M. Okamura, and E. W. Hawkes, "A Soft, Steerable Continuum Robot That Grows via Tip Extension," *Soft Robotics*, vol. 6, pp. 95–108, 2 2019.

[3] P. A. Der Maur, B. Djambazi, Y. Haberthur, P. Hormann, A. Kubler, M. Lustenberger, S. Sigrist, O. Vigen, J. Forster, F. Achermann, E. Hampp, R. K. Katzschmann, and R. Siegwart, "RoBoa: Construction and evaluation of a steerable vine robot for search and rescue applications," in *2021 IEEE 4th International Conference on Soft Robotics, RoboSoft*, pp. 15–20, IEEE, 4 2021.

[4] P. Berthet-Rayne, S. M. Sadati, G. Petrou, N. Patel, S. Giannarou, D. R. Leff, and C. Bergeles, "Mammobot: A miniature steerable soft growing robot for early breast cancer detection," *IEEE Robotics and Automation Letters*, vol. 6, pp. 5056–5063, 7 2021.

[5] S. G. Jeong, M. M. Coad, L. H. Blumenschein, M. Luo, U. Mehmood, J. H. Kim, A. M. Okamura, and J. H. Ryu, "A tip mount for transporting sensors and tools using soft growing robots," in *IEEE International Conference on Intelligent Robots and Systems*, pp. 8781–8788, IEEE, 10 2020.

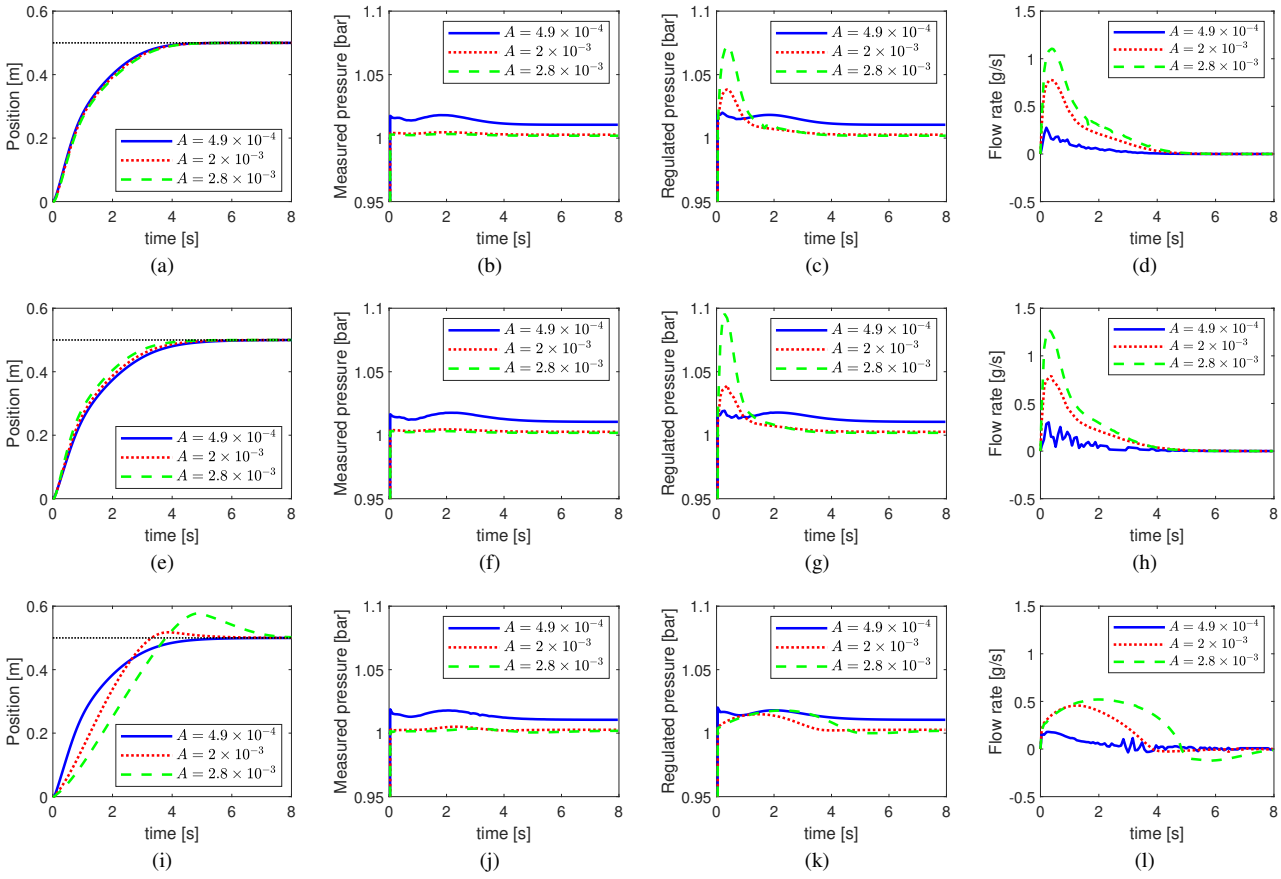

Fig. 3. Simulation results for system (2) and different values of $\boldsymbol{A}$: (a) position $\boldsymbol{x}$ with controller (14); (b) measured pressure $\boldsymbol{P}$; (c) regulated pressure $\boldsymbol{P_0}$; (d) flow rate $\boldsymbol{Q}$; (e) position $\boldsymbol{x}$ with simplified controller [17] from *Remark 2*; (f) measured pressure $\boldsymbol{P}$; (g) regulated pressure $\boldsymbol{P_0}$; (h) flow rate $\boldsymbol{Q}$; (i) position $\boldsymbol{x}$ with simplified controller (28),(29) from *Remark 3*; (j) measured pressure $\boldsymbol{P}$; (k) regulated pressure $\boldsymbol{P_0}$; (l) flow rate $\boldsymbol{Q}$.

[6] T. Takahashi, M. Watanabe, K. Tadakuma, M. Konyo, and S. Tadokoro, "Retraction Mechanism of Soft Torus Robot with a Hydrostatic Skeleton," *IEEE Robotics and Automation Letters*, vol. 5, pp. 6900–6907, 10 2020.

[7] J. D. Greer, L. H. Blumenschein, R. Alterovitz, E. W. Hawkes, and A. M. Okamura, "Robust navigation of a soft growing robot by exploiting contact with the environment," *The International Journal of Robotics Research*, vol. 39, pp. 1724–1738, 3 2020.

[8] L. H. Blumenschein, M. Koehler, N. S. Usevitch, E. W. Hawkes, D. C. Rucker, and A. M. Okamura, "Geometric Solutions for General Actuator Routing on Inflated-Beam Soft Growing Robots," *IEEE Transactions on Robotics*, pp. 1–21, 2021.

[9] L. H. Blumenschein, M. M. Coad, D. A. Haggerty, A. M. Okamura, and E. W. Hawkes, "Design, Modeling, Control, and Application of Everting Vine Robots," *Frontiers in Robotics and AI*, vol. 7, p. 153, 11 2020.

[10] C. Tutcu, B. A. Baydere, S. K. Talas, and E. Samur, "Quasi-static modeling of a novel growing soft-continuum robot," *The International Journal of Robotics Research*, vol. 40, pp. 86–98, 1 2021.

[11] A. Ataka, T. Abrar, F. Putzu, H. Godaba, and K. Althoefer, "Model-Based Pose Control of Inflatable Eversion Robot with Variable Stiffness," *IEEE Robotics and Automation Letters*, vol. 5, pp. 3398–3405, 4 2020.

[12] C. Watson, R. Obregon, and T. K. Morimoto, "Closed-Loop Position Control for Growing Robots Via Online Jacobian Corrections," *IEEE Robotics and Automation Letters*, vol. 6, pp. 6820–6827, 10 2021.

[13] H. El-Hussieny, I. A. Hameed, and J. H. Ryu, "Nonlinear Model Predictive Growth Control of a Class of Plant-Inspired Soft Growing Robots," *IEEE Access*, vol. 8, pp. 214495–214503, 2020.

[14] C. Della Santina, R. K. Katzschmann, A. Bicchi, and D. Rus, "Model-based dynamic feedback control of a planar soft robot: trajectory tracking and interaction with the environment," *The International Journal of Robotics Research*, vol. 39, pp. 490–513, 1 2020.

[15] E. Franco, A. Garriga-Casanovas, J. Tang, F. Rodriguez y Baena, and A. Astolfi, "Adaptive energy shaping control of a class of nonlinear soft continuum manipulators," *IEEE ASME Trans Mechatron*, vol. 27, pp. 280–291, 1 2022.

[16] E. Franco, "Energy Shaping Control of Hydraulic Soft Continuum Planar Manipulators," *IEEE Control Systems Letters*, vol. 6, pp. 1748–1753, 2022.

[17] E. Franco, T. Ayatullah, A. Sugiharto, A. Garriga Casanovas, and V. Vidrdyawan, "Nonlinear energy-based control of soft continuum pneumatic manipulators," *Nonlinear Dynamics*, pp. 1–25, 9 2021.

[18] M. Stolzle and C. Della Santina, "Piston-Driven Pneumatically-Actuated Soft Robots: modeling and backstepping control," *IEEE Control Systems Letters*, vol. 6, pp. 1837–1842, 2022.

[19] L. H. Blumenschein, A. M. Okamura, and E. W. Hawkes, "Modeling of Bioinspired Apical Extension in a Soft Robot," in *Living Machines 2017*, pp. 522–531, Springer, Cham, 2017.

[20] S. Joshi, H. Sonar, and J. Paik, "Flow Path Optimization for Soft Pneumatic Actuators: Towards Optimal Performance and Portability," *IEEE Robotics and Automation Letters*, vol. 6, pp. 7949–7956, 7 2021.

[21] A. Astolfi and R. Ortega, "Immersion and invariance: A new tool for stabilization and adaptive control of nonlinear systems," *IEEE Transactions on Automatic Control*, vol. 48, no. 4, pp. 590–606, 2003.

[22] G. Tao, "A simple alternative to the Barbălat lemma," *IEEE Transactions on Automatic Control*, vol. 42, no. 5, p. 698, 1997.

[23] R. Ortega, M. Spong, F. Gomez-Estern, and G. Blankenstein, "Stabilization of a class of underactuated mechanical systems via interconnection and damping assignment," *IEEE Transactions on Automatic Control*, vol. 47, pp. 1218–1233, 8 2002.

[24] H. Khalil, *Nonlinear Systems*. Upper Saddle River, NJ: Prentice-Hall, 2nd ed., 1996.